Supplementary methods

Patient and Study Design

In the first cohort, data of 73 GI cancer patients were retrospectively collected from all GI cancer patients treated with ICBs in the Department of GI Oncology, Peking University Cancer Hospital & Institute from August 1, 2015, to June 8, 2018. Eligible patients were selected based on the following criteria: 1) metastatic GI cancer patients who had failed the standard therapy; 2) patients who received at least one cycle of a programmed cell death-1 (PD-1)/program death ligand 1 (PD-L1) inhibitor (alone or combined with other agents) at Peking University Cancer Hospital (NCT02825940, NCT02978482, NCT03195478, NCT02915432, NCT03167853, NCT03472365, NCT02872116, and CTR20160872); 3) patients with complete medical information; and 4) patients with eligible tissue and blood samples. To explore genomic correlates of therapeutic efficacy, the 73 GI cancer patients were randomly assigned into the discovery (n=44) and validation (n=29) GI cohorts. Whole-exome Sequencing (WES) and RNA Immune Oncology panel sequencing analyses were performed on this dataset.

In addition, 20 patients with advanced gastric cancer who were treated with ICBs between Jan 31, 2018 and May 24, 2019 in the Department of GI Oncology, Peking University Cancer Hospital & Institute (NCT03472365, NCT03713905, NCT03736889 and NCT03667170) were included in this study as an independent GC validation cohort (Supplementary Table S1).

Details of the clinical characteristics, including the primary sites of tumors, pharmaceutical treatment, and efficacy of all patients, were recorded (Supplementary Table S1). The pathological and imaging data of all cases were reviewed retrospectively by two pathologists and two radiologists, respectively. Patients were stratified and analyzed according to the presence of a response and progression. The best response was defined as the best objective response [complete response (CR), partial response (PR), stable disease (SD), or progressive disease (PD)] assessed from the first day of treatment to progression, death, or the last follow-up. Progression-free survival (PFS) was calculated from the date of first immunotherapy administration until disease progression or death due to any cause. Overall survival (OS) was defined as the time from treatment initiation to death from any cause.

Immunohistochemical (IHC) Staining for PD-L1

Formalin-fixed paraffin-embedded (FFPE) sections were collected for immunohistochemistry (IHC) staining. To measure PD-L1 expression, anti-PD-L1 (rabbit, clone SP142, 1:100; Spring Bioscience, CA, USA) antibody was evaluated on tumor cells and tumor-infiltrating immune cells (1). Positive staining of PD-L1 was defined when ≥ 1% of the tumor/stromal cells were positive.

MMR/MSI Testing

Formalin-fixed paraffin-embedded (FFPE) sections were collected for IHC staining. To determine the microsatellite stability status, mutL homolog 1 (MLH1), mutS homolog 2 (MSH2), mutS homolog 6 (MSH6) and PMS1 homolog 2 (PMS2) were stained by using the following monoclonal antibodies: MLH1 (1:60; Clone ES05, Gene Tech, Inc., South San Francisco, CA, USA), MSH2 (1:40; Clone 25D12, Gene Tech), MSH6 (1:50; EP49, Gene Tech) and PMS2 (1:40; Clone EP51, Gene Tech). The complete loss of expression of one or more protein was considered as dMMR.

In some cases, MSI status was calculated using a single multiplex PCR, which assesses five microsatellite loci (BAT-25, BAT-26, D2S123, D5S346, and D17S250) recommended by the 1997 NCI-sponsored MSI workshop (2). For interpretation, instability at more than one locus was defined as MSI-H, instability at a single locus was defined as low MSI (MSI-L), and no instability at any locus was defined as MSS (3).

Whole-exome Sequencing and Data Preparation

We performed WES on DNA from all tumor samples along with matched blood samples and then analyzed with a mean depth of 120. Briefly, tumor DNA from FFPE specimens and matched genomic DNA from blood cells were extracted using the blackPREP FFPE DNA Kit (Analytik Jena AG, Jena, Germany) and the Tiangen Whole Blood DNA Kit (Tiangen, Beijing, PRC) according to the manufacturer's instructions. DNA concentration was quantified using the Qubit dsDNA HS Assay Kit (Life Technologies, California, USA) according to the manufacturer's recommendation. Extracted DNA was sheared into fragments with a peak at 200 bp by a Covaris M220 Focused-Ultrasonicator (Covaris, Massachusetts, USA). Fragmented DNA libraries were constructed with a KAPA HTP Library Preparation Kit (Illumina Platform) (KAPA Biosystems, Massachusetts, USA) according the manufacturer's instructions. DNA libraries were captured on a NimbleGen 44M human exome array following the manufacturer's protocols (Roche, Wisconsin, USA). The captured samples were then subjected to Illumina NovaSeq for paired-end sequencing.

Sequence reads were mapped to the reference genome (hg19) using the BWA programs (4). VarDict and FreeBayes were used for single nucleotide variant (SNV) calling, while the ANNOVAR assay was used for functional annotation of genetic variants (5, 6). To identify somatic SNV and indel mutations, the mutations in FFPE tumor samples were blanked by paired blood cell samples from patients. Somatic SNVs were selected with the following filters: (i) located in intergenic regions or intronic regions; (ii) synonymous SNVs; (iii) depth <40; (iv) allele frequency <0.03; (v) allele frequency>=0.002 in the Exome Aggregation Consortium (ExAC) database.

RNA Immune Oncology Panel Sequencing and Data Normalization

The RNA immune oncology (IO) profiling panel is a unique 398-plex gene sequencing panel that analyzes the human immune response in solid tumors (Genecast Biotechnology, Beijing, China). The panel measures 395 human genes,

which cover several cancer immune-relevant categories: immunological function and response, tumor markers, markers of tumor infiltrating cells, tumor-specific antigens, essential signaling pathways, and housekeeping (HK) genes. After RNA IO panel sequencing, we obtained 1-2 M reads per sample. Data normalization and processing were performed as previously described (7). Briefly, ten housekeeping (HK) genes were used as endogenous controls. The absolute readout of each HK gene was compared against a predetermined HK reads per million (RPM) profile. We established the baseline HK RPM profile by measuring the average RPM of a number of replicates of GM12878 cell line samples across different sequencing runs. The fold-change ratio for each HK gene: Ratio of HK = absolute read count of HK / RPM profile of HK. The median value of all HK ratios was then used as the normalization ratio for the pending sample: Normalization ratio = Median of (all HK ratios). The normalized RPM (nRPM) of all genes of an individual sample was designated as follows: nRPM of (sample S, gene G) = Absolute read count of (sample S, gene G) / Normalization ratio of (sample S). Immune scores of the described signatures were calculated as the geometric mean of gene expression belonging to the IFN-γ pathway (IFNG, IDO1, STAT1, HLA-DRA, CXCL9 and CXCL10) and the expanded immune signature (CXCL13, GZMB, IL2RG, HLA-E, CIITA, NKG7, IDO1, STAT1, LAG3, HLA-DRA, CCL5, CD3D, GZMK, TAGAP, CD3E, CXCL10, CD2, CXCR6), as previously described (8).

Immune Cell Infiltration

To compare high CNA level and low CNA level tumors, we considered the tumors having a CNA burden level within the 25th percentile (CNA-low) and the tumors having a CNA burden level higher than the 75th percentile (CNA-high). Quantitative measurements of immune cell infiltration in CNA-high or CNA-low samples were generated by single-sample Gene Set Enrichment Analysis (ssGSEA). Briefly, marker genes representing the 28 immune cell types were obtained from a recent publication (9). The abundance of each immune cell population was represented by an enrichment score. The ssGSEA score was normalized to unity distribution, for which zero is the minimum score for each immune cell type and one is the maximum score.

Study Approval

The clinical protocol for this study was approved by the Medical Ethics Committee of Peking University Cancer Hospital (Beijing, China) and was conducted according to the Declaration of Helsinki principles. All participants provided written informed consent before undergoing study procedures.

References

1. Herbst RS, et al. Predictive correlates of response to the anti-PD-L1 antibody MPDL3280A in cancer patients. *Nature*. 2014;515(7528):563-7.
2. Boland CR, et al. A National Cancer Institute Workshop on Microsatellite Instability for cancer detection and familial predisposition: development of international criteria for the determination of microsatellite instability in

colorectal cancer. *Cancer Res.* 1998;58(22):5248-57.

3. Jang M, et al. Microsatellite instability test using peptide nucleic acid probe-mediated melting point analysis: a comparison study. *BMC Cancer.* 2018;18(1):1218.
4. Li H. Aligning sequence reads, clone sequences and assembly contigs with BWA-MEM. *arXiv: Genomics.* 2014.
5. Lai Z, et al. VarDict: a novel and versatile variant caller for next-generation sequencing in cancer research. *Nucleic Acids Res.* 2016;44(11):e108.
6. Wang K, Li M, and Hakonarson H. ANNOVAR: functional annotation of genetic variants from high-throughput sequencing data. *Nucleic Acids Res.* 2010;38(16):e164.
7. Paluch BE, et al. Robust detection of immune transcripts in FFPE samples using targeted RNA sequencing. *Oncotarget.* 2017;8(2):3197-205.
8. Ayers M, et al. IFN-gamma-related mRNA profile predicts clinical response to PD-1 blockade. *J Clin Invest.* 2017;127(8):2930-40.
9. Charoentong P, et al. Pan-cancer Immunogenomic Analyses Reveal Genotype-Immunophenotype Relationships and Predictors of Response to Checkpoint Blockade. *Cell Rep.* 2017;18(1):248-62.

Supplementary Figure Legend and Figures

Figure S1. Landscape of CNAs and TMB in different GI cancer types in the first GI cancer cohort.

(A) CNA burden, **(B)** CNgain, **(C)** CNloss and (**D)** TMB in gastric cancer, colorectal cancer and other cancer types. TMB, tumor mutation burden; CNA, copy number alteration; CNgain, copy number gain; CNloss, copy number loss; GC, gastric cancer; CRC, colorectal cancer; ***, p<0.001, ****, p<0.0001.

Figure S1

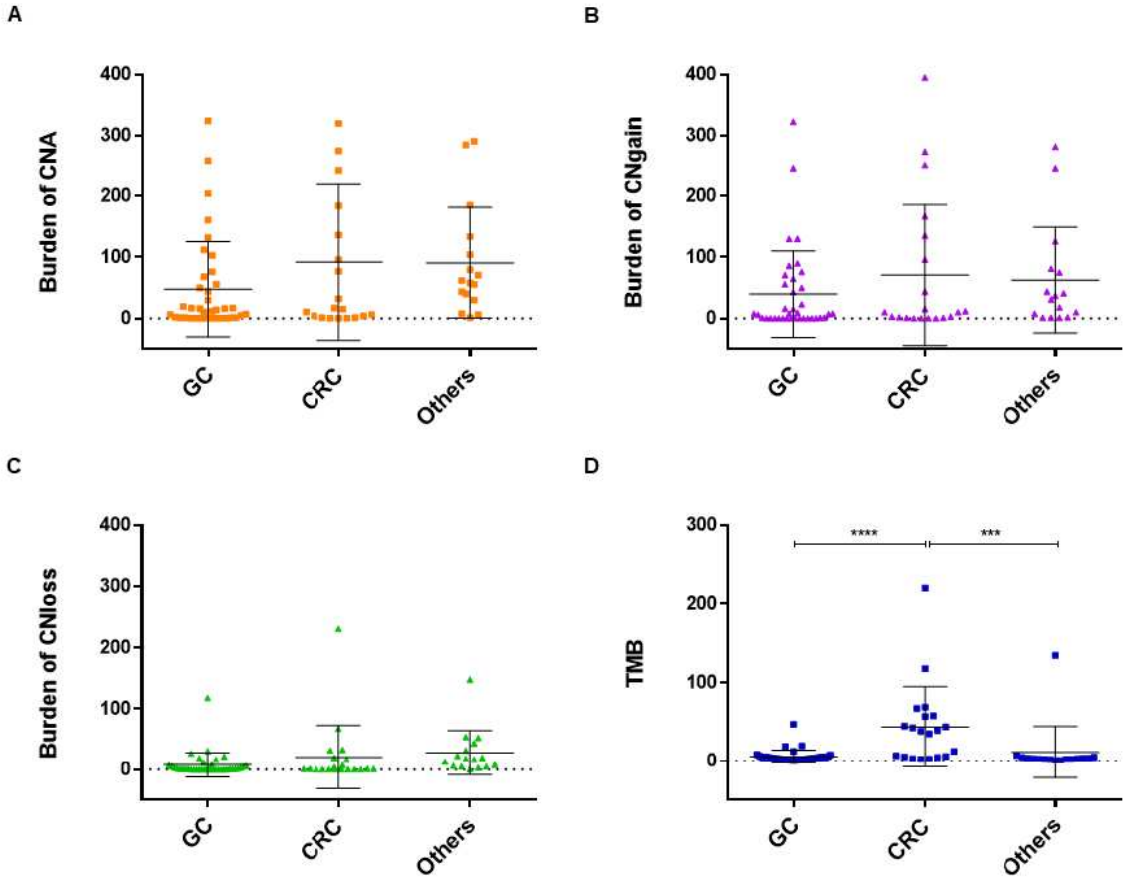

Figure S2. Association between burden of CNgain/CNloss and clinical benefit.

A. ROC curves for the prediction of clinical benefit of ICB by CNgain in the discovery cohort (n=44), the validation cohort (n=29), and the combined GI cohort (n=73).

B. ROC curves for the prediction of clinical benefit of ICB by CNloss in the discovery cohort (n=44), the validation cohort (n=29), and the combined GI cohort (n=73).

CNgain, copy number gain; CNloss, copy number loss.

Figure S2

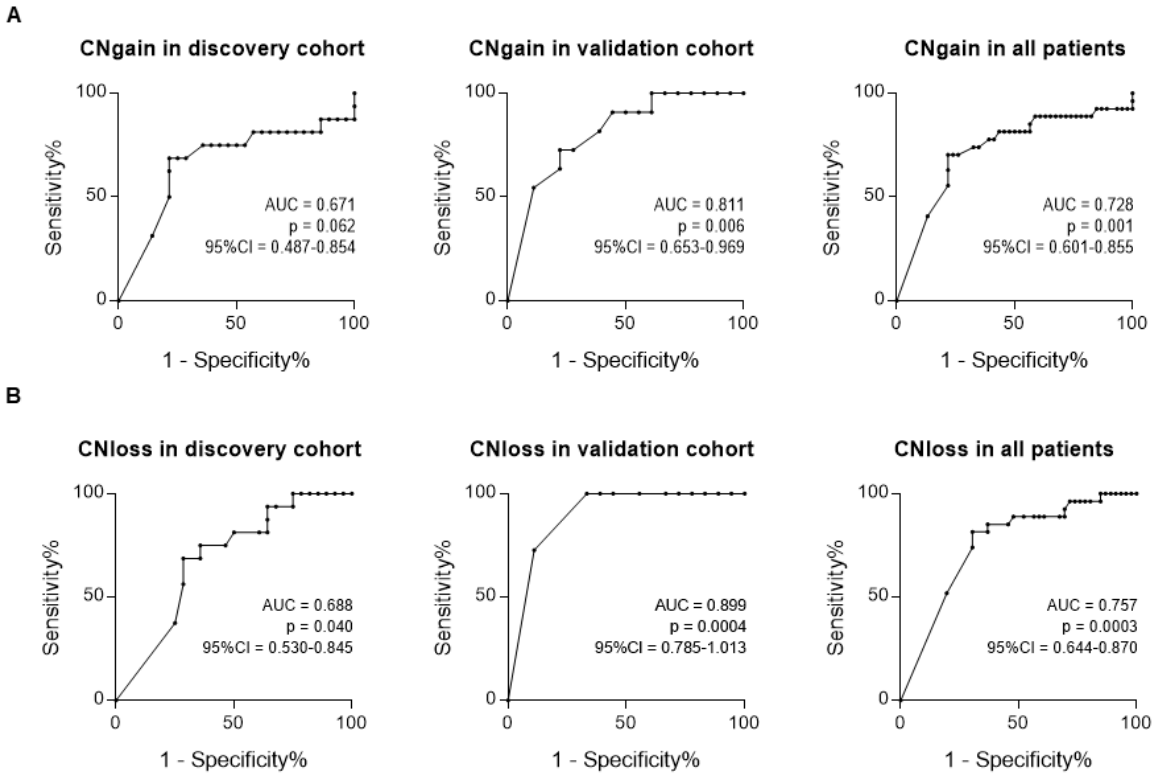

Figure S3. Association between CNgain/CNloss and overall survival.

A. Kaplan-Meier estimates of OS according to CNgain levels in the discovery cohort, validation cohort, and the combined GI cancer cohort (n=73).

B. Kaplan-Meier estimates of OS according to CNloss levels in the discovery cohort, validation cohort, and the combined GI cancer cohort (n=73).

CNgain, copy number gain; CNloss, copy number loss. The P value was calculated by the log-rank test.

Figure S3

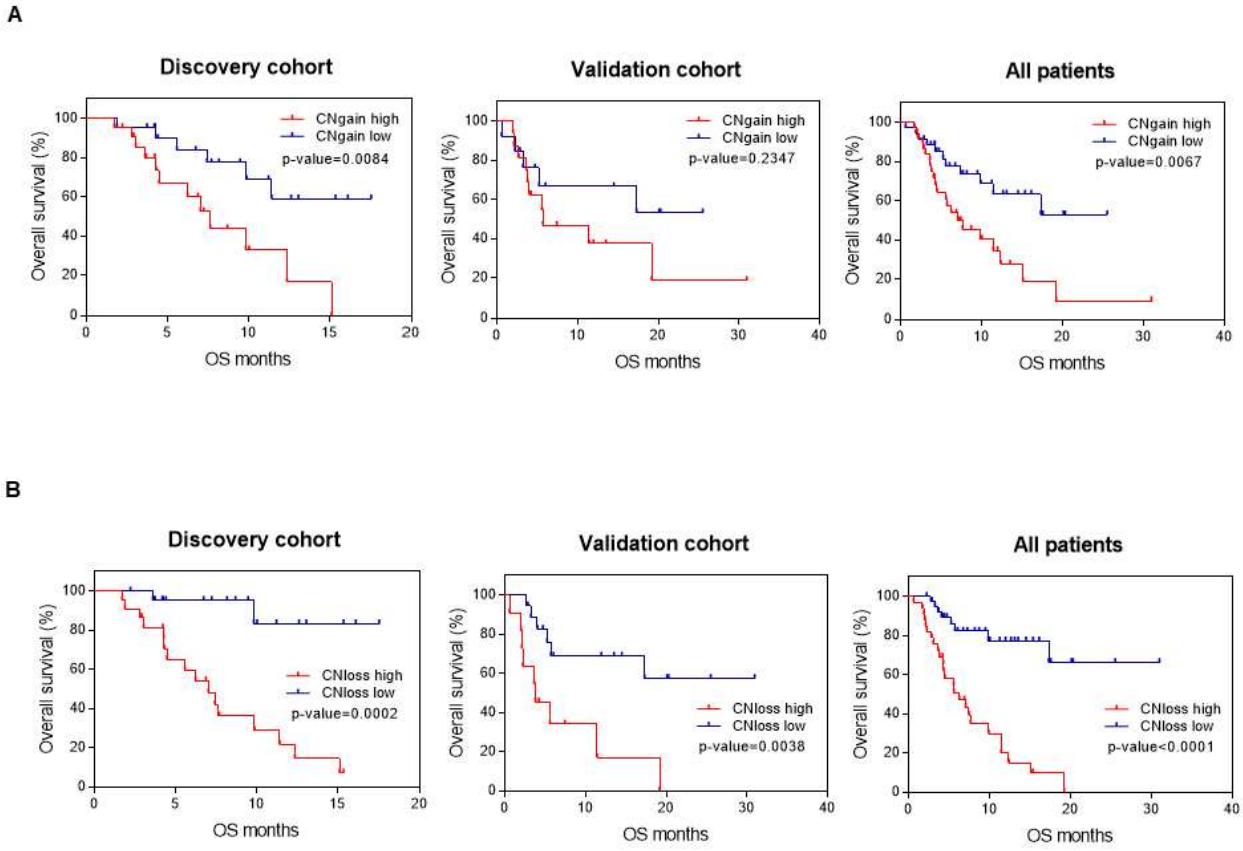

Figure S4. Association between CNgain/CNloss and progression-free survival.

A. Kaplan-Meier estimates of PFS according to CNgain levels in the discovery cohort, the validation cohort, and the combined GI cancer cohort (n=73).

B. Kaplan-Meier estimates of PFS according to CNloss levels in the discovery cohort, the validation cohort, and the combined GI cancer cohort (n=73).

The P value was calculated by the log-rank test.

Figure S4

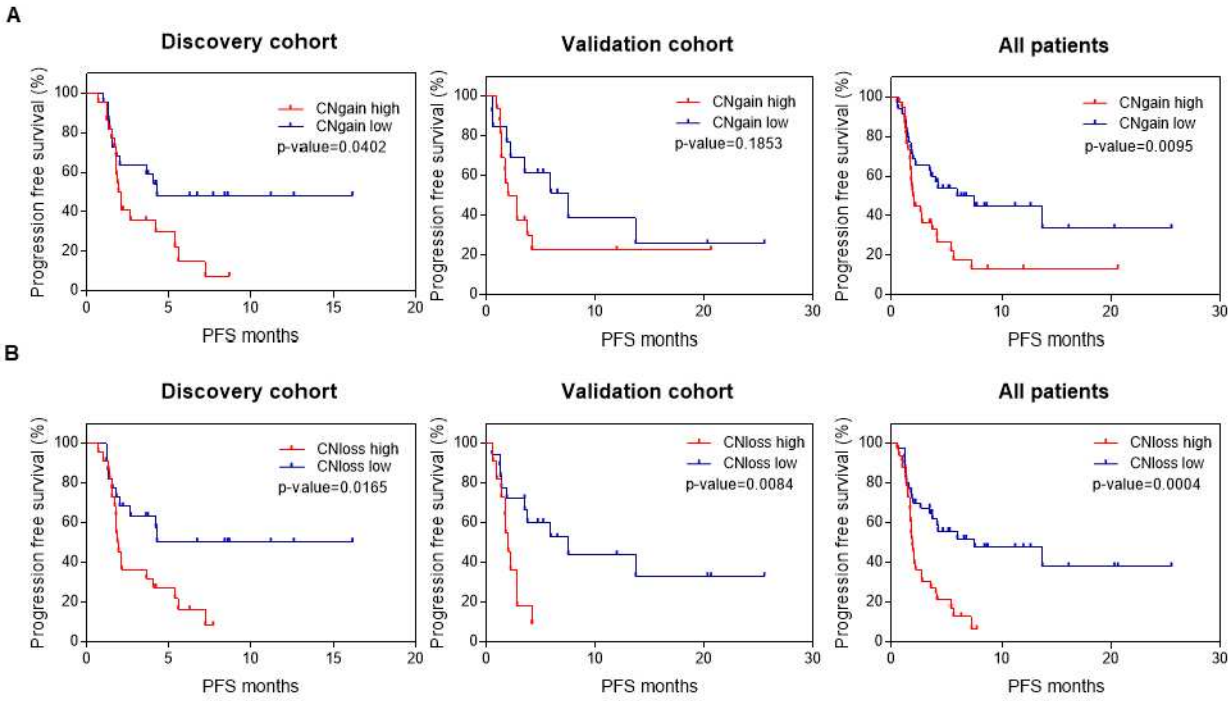

Figure S5. Validation of CNA burden and TMB in an independent gastric cancer (GC) cohort.

A. Rate of DCB in CNA low and high subgroups (fisher's exact test, *P* value<0.05).

B. Rate of DCB in TMB low and high subgroups.

C. Proportions of patients with DCB calculated within each of the four indicated subgroups.

D. Waterfall plot of tumor response to ICB according to the CNA burden (CNA-low, grey bar; CNA-high, red bar) and TMB (asterisk). The Y axis represents the percentage of maximum tumor reduction assessed according to the RECIST 1.1 criteria.

Figure S5

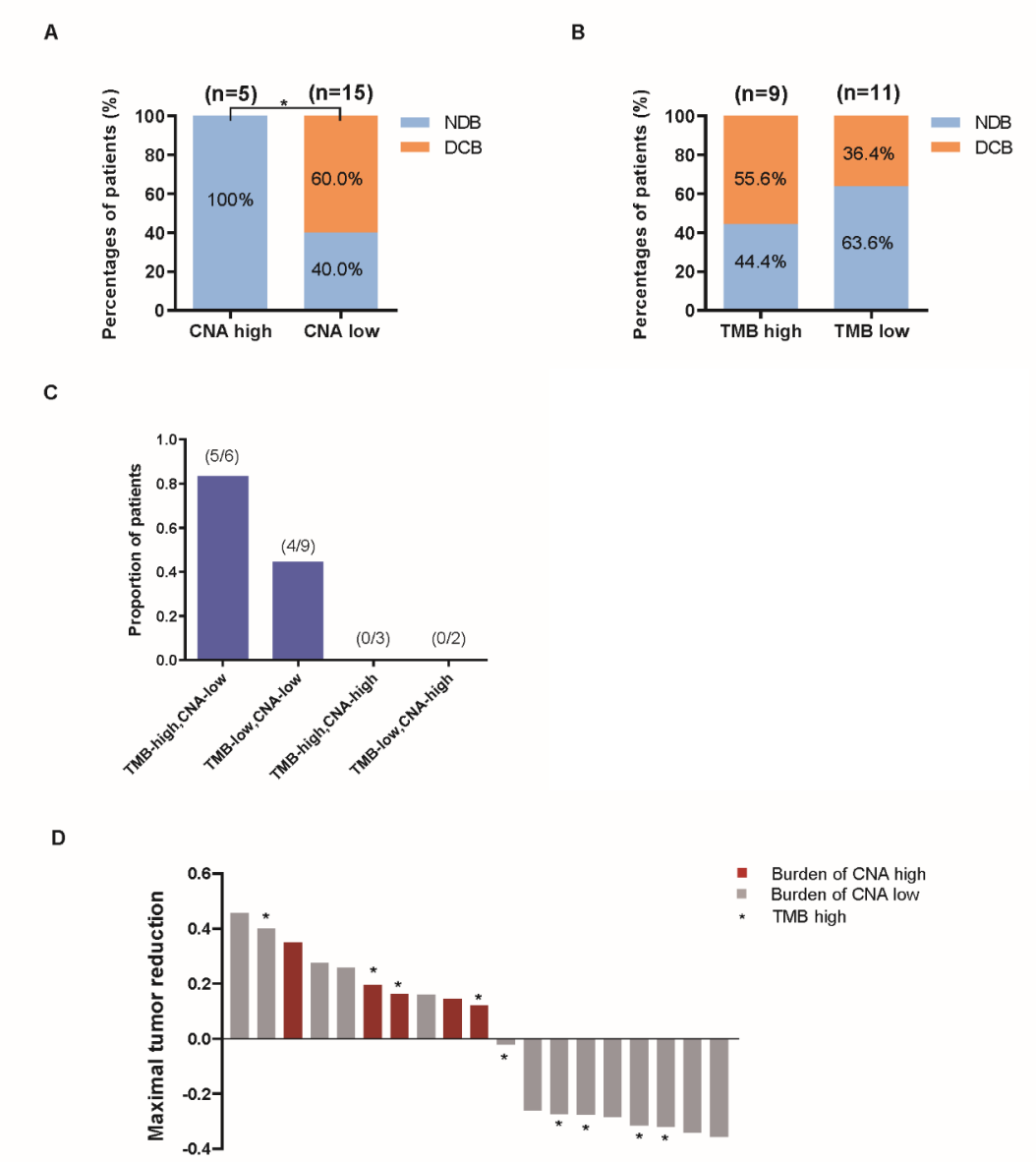

Figure S6. The correlation of the CNA burden and immune phenotypes.

A. Single-sample Gene Set Enrichment Analysis (ssGSEA) identifying the relative infiltration of immune cell populations with available TCGA RNA-Seq data for upper and lower CNA burden level in gastric cancer (left) and colon cancer (right), respectively.

B. Significantly enriched immune cell populations in CNA-low versus CNA-high in both gastric cancer (left) and colorectal cancer (right) TCGA data sets.

P value<0.05. lower, lower quartile value; upper, upper quartile value; CNA-low, copy number alteration low; CNA-high, copy number alteration high; STAD, stomach adenocarcinoma; COAD, colon adenocarcinoma.

Figure S6

A

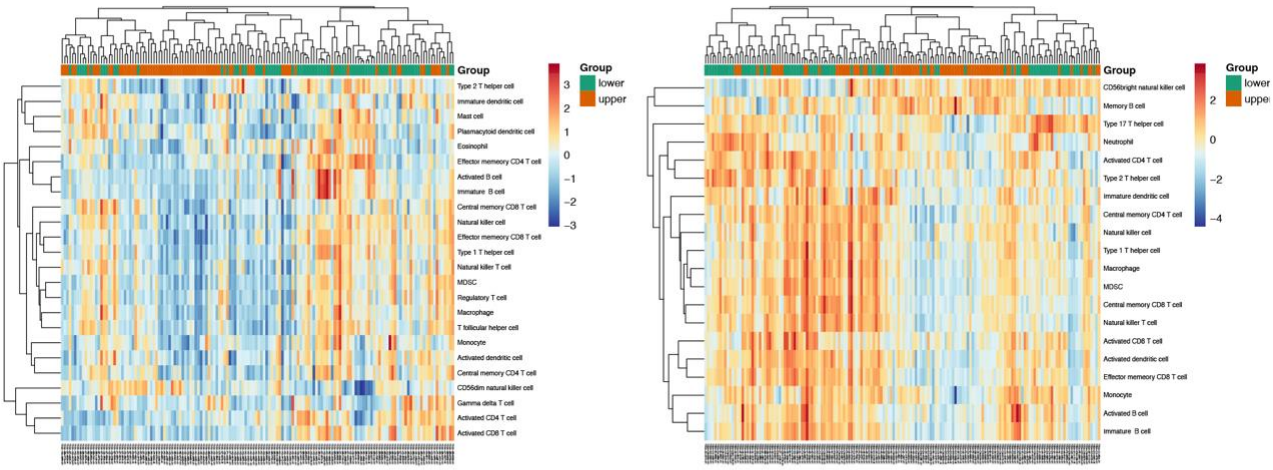

B

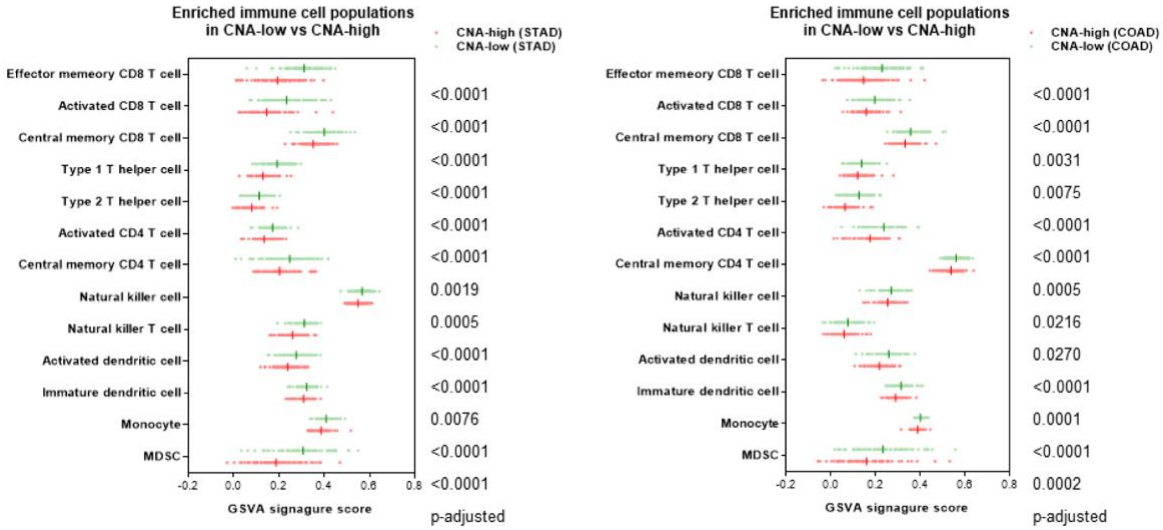

Table S1 Baseline characteristics.

Factors		Discovery GI cohort (n=44)	Validation GI cohort (n=29)	Independent GC cohort (n=20)
Age				
	median (range)	56 (23.0-76.0)	61 (15.0-76.0)	62.5 (41.0-76.0)
	<60	25 (56.8%)	13 (44.8%)	8 (40%)
	≥60	19 (43.2%)	16 (55.2%)	12 (60%)
Gender				
	Male	32 (72.7%)	20 (69.0%)	15(75%)
	Female	12 (27.3%)	9 (31.0%)	5(25%)
Race				
	Asian	44 (100%)	29 (100%)	20 (100%)
Cancer type				
	Gastric cancer (GC)	20 (45.5%)	17 (58.6%)	20 (100%)
	Colorectal cancer (CRC)	13 (29.5%)	7 (24.2%)	-
	Others[a]	11 (25%)	5 (17.2%)	-
Treatment option				
	Anti-PD-1 therapy	24 (54.5%)	23 (79.4%)	15 (75%)
	Anti-PD-L1 therapy	12 (27.3%)	3 (10.3%)	3 (15%)
	Combo	8[b] (18.2%)	3[c] (10.3%)	2[d] (10%)
No. of prior lines of therapy (Median=1)				
	0	6 (13.6%)	6 (20.7%)	2 (10%)
	1	16 (36.4%)	9 (31.0%)	8 (40%)
	>1	22 (50%)	14 (48.3%)	10 (50%)
Types of therapy prior to ICB				
	Chemotherapy	37 (84.1%)	22 (75.9%)	18 (90%)
	Targeted therapy	11 (25%)	7 (24.1%)	5 (25%)
	Radiotherapy	4 (9.1%)	-	1 (5%)
Tumor MSI status				
	MSI-H/dMMR	14 (31.8%)	8 (27.6%)	3 (15%)
	MSI-L/MSS/pMMR	19 (43.2%)	16 (55.2%)	17 (85%)
	NA	11 (25%)	5 (17.2%)	0 (0%)
PD-L1 expression				
	Positive	8 (18.2%)	13 (44.8%)	5 (25%)
	Negative	18 (40.9%)	6 (20.7%)	14 (70%)
	NA	18 (40.9%)	10 (34.5%)	1 (5%)

[a] Other types of tumors include pancreatic neuroendocrine tumors (PanNETs), gastrointestinal-NETs and cholangiocellular carcinoma. [b] One patient received PD-1 blockade plus chemotherapy, and one patient received PD-1 blockade plus Apatinib. [c] Two patients received PD-1 blockade plus chemotherapy. [d] Two patients received PD-1 blockade plus Apatinib.

Table S2 Characteristics and clinical benefit rate in the GI cancer cohort (n=73).

Characteristics		No. of patients	Clinical benefit		P value
			DCB	NDB	
MSI/MMR status		57			
	MSI-H/dMMR	22	13 (59.1%)	9 (40.9%)	
	MSI-L/MSS/pMMR	35	10 (28.6%)	25 (71.4%)	0.022
PD-L1 expression		45			
	PD-L1-	24	9 (37.5%)	15 (62.5%)	
	PD-L1+	21	7 (33.3%)	14 (66.7%)	0.771
TMB		73			
	TMB>5	30	18 (60.0%)	12 (40.0%)	
	TMB<=5	43	9 (20.9%)	34 (79.1%)	0.001
CNA		73			
	CNA<=10	29	20 (69.0%)	9 (31.0%)	
	CNA>10	44	7 (15.9%)	37 (84.1%)	<0.001
CNgain		73			
	CNgain<=8	35	20 (57.1%)	15 (42.9%)	
	CNgain>8	38	7 (18.4%)	31 (81.6%)	0.001
CNloss		73			
	CNloss<=4	40	23 (57.5%)	17 (42.5%)	
	CNloss>4	33	4 (12.1%)	29 (87.9%)	<0.001